Supporting Online Material
Materials and Methods
Supplementary Text
figs. S1-S14
table S1
References

Materials and Methods

Mice

The following mice were purchased from the Jackson Laboratory, and maintained at the University of Chicago under specific-pathogen free conditions: C57BL/6J (B6) mice, CD45.1/.1 B6.SJL-*Ptprc*^{a} *Pepc*^{b}/BoyJ mice, TRAMP C57BL/6-Tg(TRAMP)8247Ng/J mice, *Rag1*-deficient B6.129S7-*Rag1*^{tm1Mom}/J mice, and Aire-deficient B6.129S2-Aire$^{tm1.1Doi}$/J mice. OT-II transgenic C57BL/6-Tg(TcraTcrb)425Cbn/Crl mice were purchased from Charles River. Foxp3^{gfp} reporter mice (*6*) were a generous gift from Alexander Rudensky. MJ23tg mice, RT83tg mice, and TCRβtg mice were generated at the University of Chicago Transgenic Core Facility. All mice were bred and maintained in accordance with the animal care and use regulations of the University of Chicago.

Generation of TCR transgenic mice

TCR transgenic mice were generated by standard methods using the TCR cassette vectors of Kouskoff et al. (*25*). The TCR cassette vectors pTαcass and pTβcass were a gift from C. Benoist. The TCR chains are as follows, with the CDR3 amino acid sequences indicated.

a) "TCRβtg" mice:
Vβ3(TRBV26)-ASSLGSSYEQY, utilizing TRBJ2-7
b) "MJ23tg" mice:
Vα2(TRAV14D-3)-LYYNQGKLI, utilizing TRAJ23
Vβ3(TRBV26)-ASSLGSSYEQY, utilizing TRBJ2-7
c) "RT83tg" mice:
Vα8(TRAV12D-3)-ALRDSNNRIF, utilizing TRAJ31
Vβ3(TRBV26)-ASSLGSSYEQY, utilizing TRBJ2-7

The rearranged TCRα and TCRβ chains were cloned into pTαcass and pTβcass, respectively. Rearranged TCRα chains was generated by gene synthesis (Genscript), and cloned into the XmaI/SacII sites of the pTαcass vector using STBL4 cells (Invitrogen). The resulting TCRα constructs were excised from the vector using SalI. The rearranged TCRβ chain was generated via splicing by overlap extension, cloned into pBSII (Stratagene) using XhoI/SacII sites, and subcloned into pTβcass using STBL4 cells. The resulting TCRβ construct was excised from the vector using KpnI. Excised linear TCRα and TCRβ constructs were purified and either injected singly (for TCRβtg) or co-injected (for MJ23tg and RT83tg) into blastocysts using standard methods. Transgenic mice were generated on either a pure B6 background or on a (CBA x B6)F2 background and crossed to the B6 background for at least 12 generations. Genotyping of transgenic mice was performed by PCR amplification of earpunch DNA using the following primers:

Vα2(TRAV14D-3)-LYYNQGKLI forward 5'-CGGGGGGAATGGACAAGATC-3'
Vα2(TRAV14D-3)-LYYNQGKLI reverse 5'-AAAGATAAGCTTCCCCTGGTTATAATAGAG-3'

Vα8(TRAV12D-3)-ALRDSNNRIF forward 5'-CATCTCCCGGGGGGAATGCGTC-3'
Vα8(TRAV12D-3)-ALRDSNNRIF reverse 5'-AGATTCTGTTATTGCTATCTC-3'
Vβ3(TRBV26)-ASSLGSSYEQY forward 5'-CCAGTATCTCGAGCGGATGG-3'
Vβ3(TRBV26)-ASSLGSSYEQY reverse 5'-TTCATAGGAGCTACCCAGAC-3'

TCR CDR3 length distribution analysis

T cells were FACS-sorted into TRI reagent (Sigma), and RNA was isolated by standard methods using glycogen (Roche) as a carrier for precipitation. RNA was reverse transcribed using oligo dT primer (IDT) and Superscript II reverse transcriptase (Invitrogen). cDNA was subjected to PCR amplification with Platinum Taq (Invitrogen) using a 6-FAM-labeled Cα-specific primer (5'-CCATGGTTTTCGGCACATTG-3') paired with a Vα2(TRAV14)-specific primer (5'-GAGAAAAAGCTCTCCTTGCAC-3'). 40 cycles of PCR amplification were performed with annealing at 55°C. Amplification products were resolved and quantified on an Applied Biosystems 3730XL automated sequencer, using an internal calibration control to determine fragment length. CDR3 size spectra and peak areas were analyzed using Peak Scanner software (Applied Biosystems).

TCR sequence analysis

For the sequence analysis of Vα2(TRAV14)$^+$ TCRα or Vβ3(TRBV26)$^+$ TCRβ chains, cDNA from FACS-sorted T cell subsets was PCR-amplified using the following primers. The forward fusion primers follow the sequence PrimerA-Barcode-mVregion, and the reverse fusion primers follow the sequence PrimerB-Barcode-mCregion. Sequences are as follows:

PrimerA 5'-CCATCTCATCCCTGCGTGTCTCCGACTCAG-3'
PrimerB 5'-CCTATCCCCTGTGTGCCTTGGCAGTCTCAG-3'
mVα2.P2 5'-GAGAAAAAGCTCTCCTTGCAC-3'
mCα.P2 5'-CCATGGTTTTCGGCACATTG-3'
mVβ3.P1 5'-CCTTGCAGCCTAGAAATTCAG-3'
mCβ.P1 5'-CTTGGGTGGAGTCACATTTCTC-3'

The barcodes used were those recommended by the manufacturer for use with GS FLX Titanium emPCR (LIB-L) chemistry (Roche). PCR amplicons were gel-purified using a Gel Extraction Kit (Qiagen), and samples were processed for sequencing. Sequencing was performed at the Utah State University Center for Integrated Biosystems using the Titanium sequencing chemistry on a Roche GS FLX system. The use of barcoded samples permitted the multiplexing of up to 14 different samples.

TCR data analysis. Each sequence read was processed using a custom written python script (available upon request) to demultiplex the sample barcodes and parse out and translate the CDR3 regions. Using the parsed CDR3 sequences we generated a count table which had for each CDR3 and each sample a count of how many times that CDR3 element appeared. Typically, 1000-2000 sequence reads were obtained per sample.
TCR repertoire analysis. To analyze the repertoire similarity CDR3 elements we used the Morisita-Horn Similarity Index (*11*). The index computes the similarity between two populations of "species", originally taxonomic species, but here CDR3 species. If x_i is the number of time species "i" occurs in sample X and y_i the number in sample Y then the index is defined as:

$$C_H = \frac{2\sum_{i=1}^{S} x_i y_i}{\left(\frac{\sum_{i=1}^{S} x_i^2}{X^2} + \frac{\sum_{i=1}^{S} y_i^2}{Y^2}\right) XY}$$

Where X is the sum of x_i, Y is the sum of y_i and S is the number of species. The resulting matrix of pair-wise similarities between all samples was then clustered using standard hierarchical clustering using 1-C_H as the distance metric and using average linkage for the joining.

Antibodies, flow cytometry, and fluorescence-activated cells sorting

All antibodies used were purchased from eBioscience, Biolegend, and BD Biosciences. Cells were stained with the following conjugated antibodies: CD4 (GK1.5), CD8α (53-6.7), CD44 (IM7), CD45.1 (A20), CD45.2 (104), CD11c (N418), and F4/80 (BM8). Typically, cells were stained for 20 minutes on ice in staining buffer (phosphate-buffered saline with 2% FCS, 0.1% NaN_3, 5% normal rat serum, 5% normal mouse serum, 5% normal rabbit serum (all sera from Jackson Immunoresearch), and 10 μg/mL 2.4G2 antibody). Intracellular staining for Foxp3 was performed using clone FJK-16s and fixation/permeabilization buffers from eBioscience. Neuropilin-1 expression was assessed using polyclonal goat IgG antibody (R&D Systems) coupled with rabbit anti-goat secondary antibody (Invitrogen). Flow cytometry was performed on an LSR-II flow cytometer (BD Biosciences), using FlowJo data analysis software (Tree Star). Fluorescence-activated cell sorting was performed using a FACSAria (BD Biosciences).

Generation of mixed bone marrow chimeric mice

$CD45^{.2/.2}$ recipient mice were treated with sublethal doses of radiation (500 rads) one day prior to transfer. Bone marrow cells from donor mice were harvested and depleted of T cells using CD90.2 MACS beads (Miltenyi). 5 x 10^6 cells were then injected by tail vein injection into host mice. Donor cells consisted of cells isolated from MJ23tg *Rag1*$^{-/-}$ $CD45.1^+$ female donor mice mixed with polyclonal "filler" cells from $CD45^{.2/.2}$ B6 females. A mixture of 5% MJ23tg cells to 95% filler cells consistently resulted in a clonal frequency of MJ23tg thymocytes of less than 1%. 6 weeks post-engraftment, the fate of MJ23tg cells was analyzed. For experiments utilizing *Aire*$^{+/+}$ or *Aire*$^{-/-}$ recipients, "filler" cells were isolated from *Aire*$^{-/-}$ females.

T cell transfer experiments

$CD4^+$ T cells isolated from MJ23tg *Rag1*$^{-/-}$ $CD45.1^+$ female donor mice were purified using MACS sorting (Miltenyi), and 1 x 10^5 cells were transferred intravenously into 5-month-old $TRAMP^{+/+}$ or B6 recipients. 30 days post-transfer, the fate of donor cells was assessed.

T cell stimulation experiments

Prostates from 20-27-week-old TRAMP mice were dissected and injected with a solution containing liberase CI / DNase I (Roche). Tissue was then mechanically disrupted, and the immune cell fraction was enriched on a continuous Percoll (GE Healthcare) gradient. $CD45^+CD11c^+F4/80^{neg}$ cells from this fraction were then purified by FACS. Cell cultures were set up in 96-well round-bottom plates coated with collagen (Sigma). Cultures contained 3 x 10^4 $CD45^+CD11c^+F4/80^{neg}$ cells, 3 x 10^4 $CD4^+Foxp3^{neg}$ MJ23tg T cells or OT-IItg cells labeled with CFSE (Molecular Probes), and 100 U/mL recombinant mouse IL-2 (Miltenyi). In addition, anti-MHC-II antibody clone M5 (eBioscience) or isotype control antibody was added to the culture at a final concentration of 10 μg/mL. Dilution of CFSE was assessed by flow cytometry on day 4.

Treg suppression assays

Cultures containing the following components were established in 96 well round-bottom

plates: a) 5 x 10^4 irradiated (3000 rads) splenocytes, b) 2.5 x 10^4 $CD4^+CD25^{neg}$ polyclonal "T responder" cells labeled with CellTrace-Violet dye (Invitrogren), c) either 2.5 x 10^4 $CD4^+CD25^{neg}$ or 2.5 x 10^4 $CD4^+CD25^+$ T cells isolated from polyclonal or MJ23tg $Rag1^{-/-}$ males, and d) 0.25 μg/mL soluble anti-CD3 antibody clone 145-2C11 (BioXCell). Dilution of CellTrace-Violet dye by T responder cells was assessed by flow cytometry on day 4.

Statistical Analysis

Data were analyzed using Prism software (GraphPad). For the comparison of two groups, either the Student's t-test (two-tailed) or the nonparametric Mann-Whitney test were used, depending on whether data were normally distributed. For comparisons of multiple groups, one-way ANOVA was employed, coupled with Tukey's HSD post-hoc tests when appropriate.

Supplementary Text

Expression of neuropilin-1 on MJ23 and polyclonal Tregs

Recent reports suggest that induced Tregs of extrathymic origin express low amounts of the marker neuropilin-1 (Nrp-1) (*26, 27*). Flow cytometric analyses of $Foxp3^+$ MJ23tg Tregs in the lymph nodes and spleen of MJ23tg bone marrow chimeric mice revealed high expression of Nrp-1 by these cells (fig. S7). Moreover, polyclonal T cells from the prostates of tumor-free B6 or tumor-bearing TRAMP mice exhibited unimodal, intermediate expression of Nrp-1 (fig. S8). Comparatively, many Tregs from the colon, which is thought to contain a substantial proportion of induced Tregs (*28*), expressed low amounts of Nrp-1 (fig. S8). Together, these data are suggestive of a thymic origin for both MJ23 Tregs and polyclonal prostate tumor-infiltrating Tregs, consistent with our data demonstrating that the MJ23 TCR facilitates Treg development in the thymus (Fig. 3).

Factors limiting the recovery of donor MJ23 Tregs from the prostate of chimeric mice

Data presented in Fig. 1 demonstrate that endogenous Tregs expressing the MJ23 TCR are recurrently enriched in TRAMP prostate tumors. However, in MJ23tg bone marrow chimeric mice generated in B6 or TRAMP male hosts, donor-derived MJ23tg Tregs were often not enriched in the prostate (Fig. 3, A and C). This effect was likely the result of two factors associated with the experimental approach utilized to generate chimeric mice, in which cells from MJ23tg mice were engrafted, along with an excess of polyclonal "filler" cells, into sublethally irradiated polyclonal hosts. First, chimeric mice exhibited a marked decrease in the total number of Tregs in the prostate relative to unmanipulated mice (fig. S11A). These data indicate that radiation alters the prostatic Treg infiltrate, and induces a substantial reduction in the quantity of Tregs recovered. Second, prostatic infiltration by donor-derived MJ23tg cells was likely limited by competition with host-derived polyclonal MJ23 Tregs. In this scenario, endogenous Tregs that survive sublethal irradation may occupy putative antigenic niches in the prostate, thereby restricting infiltration by donor-derived MJ23tg T cells that enter the peripheral pool following a time lag required for bone marrow engraftment and T cell development in the thymus. In support of this hypothesis, when MJ23tg bone marrow chimeras were analyzed at a later time point (20 weeks post-engraftment), donor-derived MJ23tg Tregs were observed in the prostates of B6 male hosts (fig. S11B), indicating that donor-derived MJ23tg Tregs access the prostate at later time points.

figs. S1-S14

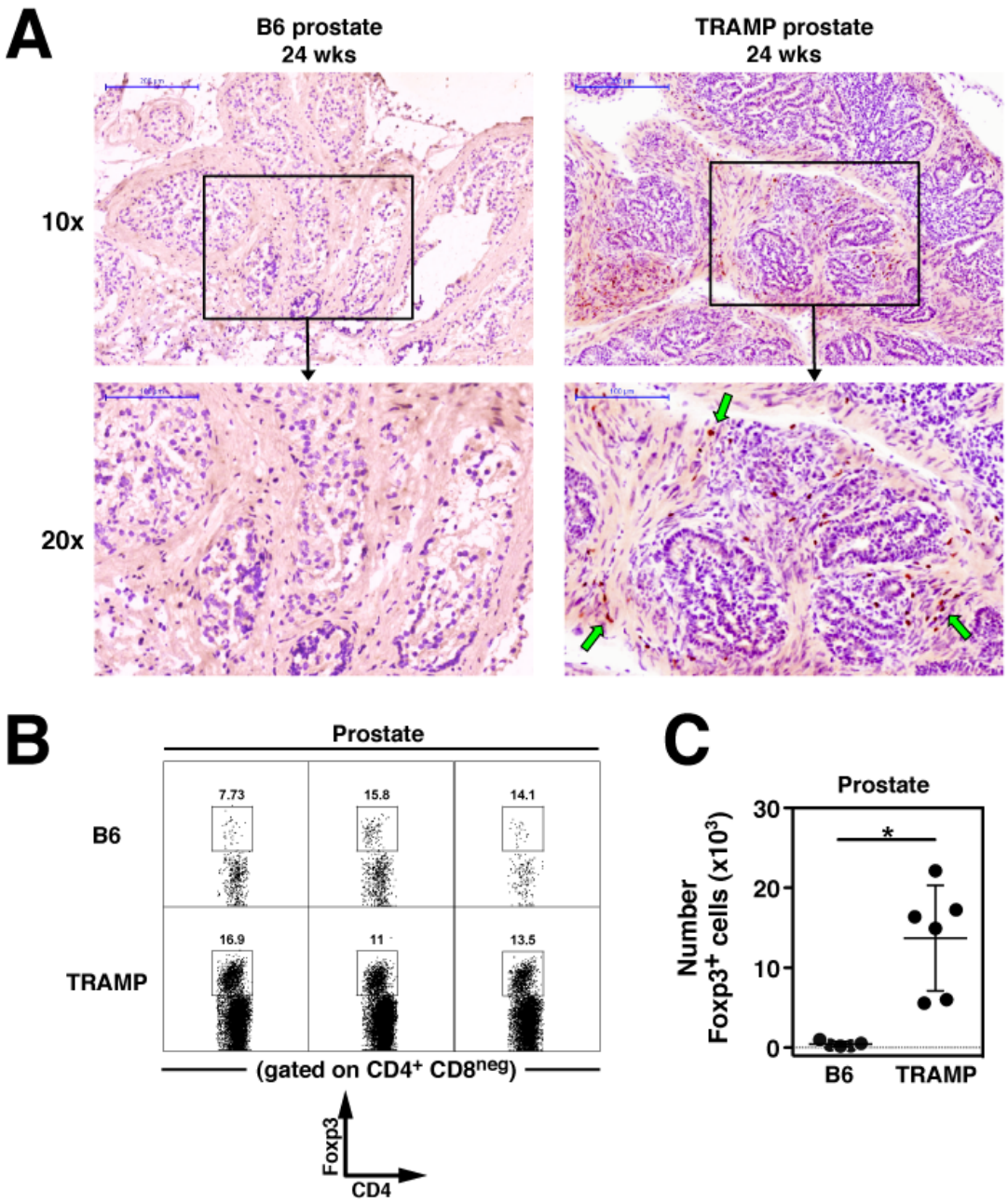

fig. S1. Enrichment of Tregs in TRAMP prostate tumors. (A) Immunohistochemical analysis of Foxp3 expression in the prostatic dorsolateral lobes of 24-week-old B6 and TRAMP mice. Magnification is indicated. Green arrows denote Foxp3-expressing cells. **(B)** Representative flow cytometric analysis of Foxp3 expression by $CD4^+$ T cells isolated from the prostates of 24-week-old B6 and TRAMP mice. **(C)** Quantification of the absolute number of $Foxp3^+CD4^+$ cells isolated from 24-week-old B6 and TRAMP prostates. The mean ± SEM is indicated. The asterisk denotes $p < 0.05$.

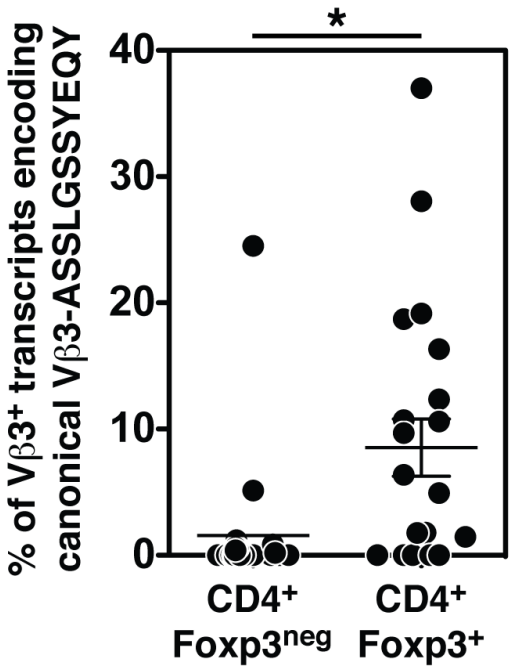

fig. S2. Identification of a canonical TCRβ chain recurrently expressed by Tregs infiltrating TRAMP prostate tumors. $CD4^{+}Foxp3^{neg}$ and $CD4^{+}Foxp3^{+}$ T cells were FACS-purified from the prostates of ~27-week-old male $TRAMP^{+/-}$ $Foxp3^{gfp}$ mice, and $V\beta3^{+}$ TCRβ transcripts were PCR-amplified and subjected to deep sequencing. The analysis identified a canonical $V\beta3^{+}$ TCRβ chain of CDR3 sequence ASSLGSSYEQY that was recurrently expressing by $CD4^{+}Foxp3^{+}$ T cells. For each sample, the percentage of all $V\beta3^{+}$ TCRβ transcripts encoding the canonical Vβ3-ASSLGSSYEQY chain is plotted. The mean ± SEM is indicated. The asterisk denotes $p < 0.05$. For simplicity, transgenic mice expressing the canonical TCRβ chain are referred to as "TCRβtg" mice. Data are pooled from $N = 5$ independent FACS sorting experiments.

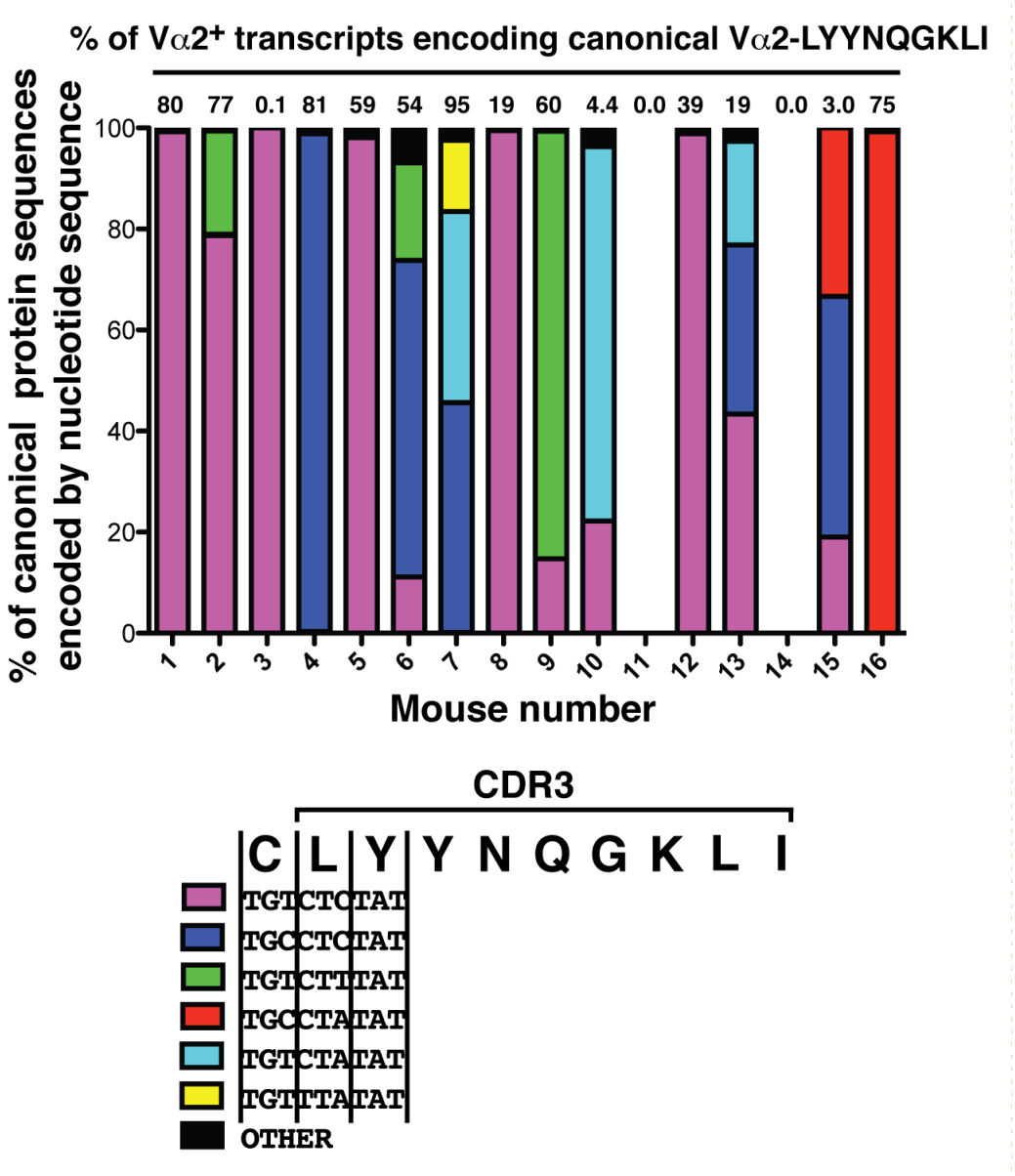

fig. S3. In many TRAMP$^{+/-}$ Foxp3^{gfp} TCRβtg mice, the canonical Vα2-LYYNQGKLI chain is encoded by a single nucleotide sequence. Data are from the same mice presented in Fig. 1. There are six possible nucleotide sequences that encode the canonical Vα2-LYYNQGKLI chain (indicated by different colors). These nucleotide sequences vary only at the codons encoding the conserved cysteine N-terminal to the CDR3, and the leucine and tyrosine at the first two CDR3 positions. Nucleotides encoding the remaining YNQGKLI residues are invariant because they are derived from the TRAJ23 segment. Across the top, for each mouse, the percentage of Vα2^{+} transcripts that encode the canonical Vα2-LYYNQGKLI is indicated. The distribution of nucleotide sequences encoding these canonical chains is indicated in the colored bar graphs. For example, for mouse #1, 80% of Vα2^{+} transcripts encode the canonical Vα2-LYYNQGKLI chain, and >99% of these are encoded by the magenta nucleotide sequence. Data are pooled from *N* = 3 independent FACS sorting experiments.

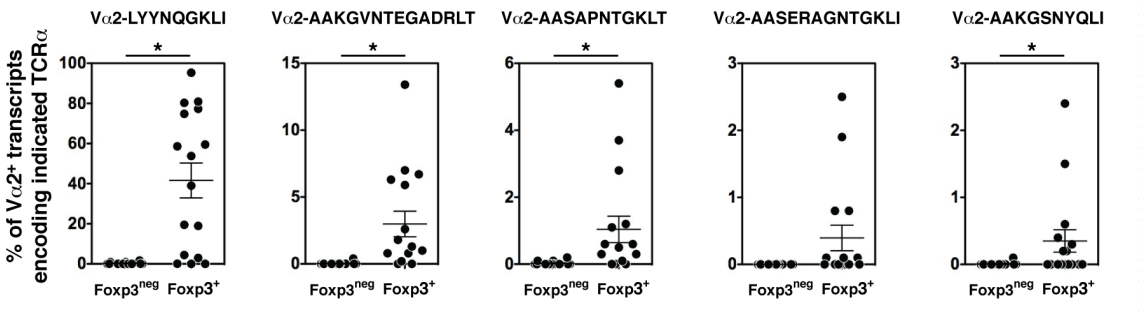

fig. S4. Five most common Vα2$^+$ TCRα chains expressed by prostatic CD4$^+$Foxp3$^+$ T cells from TRAMP$^{+/-}$ Foxp3^{gfp} TCRβtg mice. Analysis of Vα2 (TRAV14)$^+$ TCRα chains in tumor-bearing TRAMP$^{+/-}$ Foxp3^{gfp} TCRβtg mice. Data are from the same mice presented in Fig. 1B. CD4$^+$Foxp3^{neg} and CD4$^+$Foxp3$^+$ T cells were FACS-purified from the prostates of ~27-week-old male mice, and Vα2$^+$ TCRα transcripts were PCR-amplified and subjected to deep sequencing. The percentage of all Vα2$^+$ TCRα transcripts encoding the indicated TCRα chain is plotted. The mean ± SEM is indicated. Asterisks indicate $p < 0.05$. Data are pooled from $N = 3$ independent FACS sorting experiments.

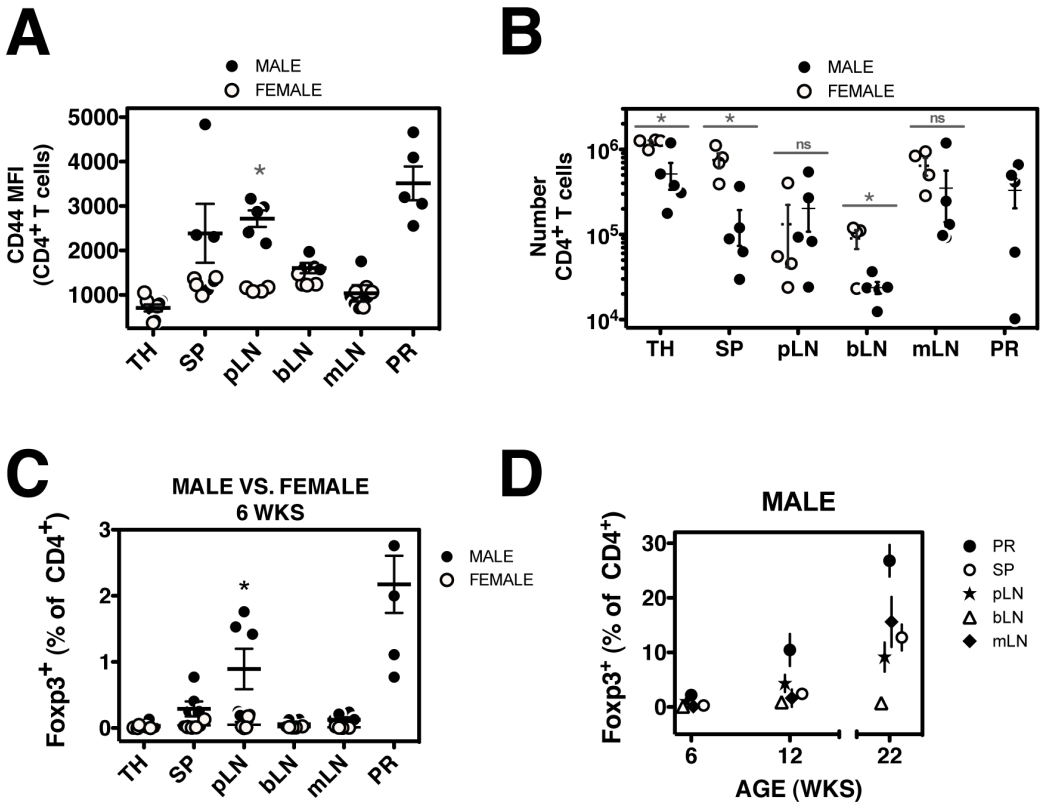

fig. S5. Analysis of CD4$^+$Foxp3$^+$ T cells in MJ23tg *Rag1*$^{-/-}$ mice. Data are from the same mice presented in Fig. 2. TH, thymus; SP, spleen; pLN, periaortic lymph nodes; bLN, brachial lymph nodes; mLN, mesenteric lymph nodes; PR, prostate. **(A)** Summary plot of the mean fluorescence intensity (MFI) of staining for the CD44 activation marker on CD4$^+$ T cells isolated from the indicated organs of 6-week-old male and female mice. **(B)** Summary plot of the absolute number of CD4$^+$ T cells from different anatomical sites of 6-week-old male or female mice. **(C)** Summary plot of the frequency of Foxp3$^+$ cells (as a percentage of CD4$^+$ cells) from the indicated organs of 6-week-old male and female mice. **(D)** Summary plot of the frequency of Foxp3$^+$ cells (as a percentage of CD4$^+$ cells) from the indicated organs of male mice of various ages. The mean ± SEM is indicated. Asterisks indicate $p < 0.05$, for comparisons of males vs. females at a given anatomical site. Data are pooled from $N = 2$ independent analyses.

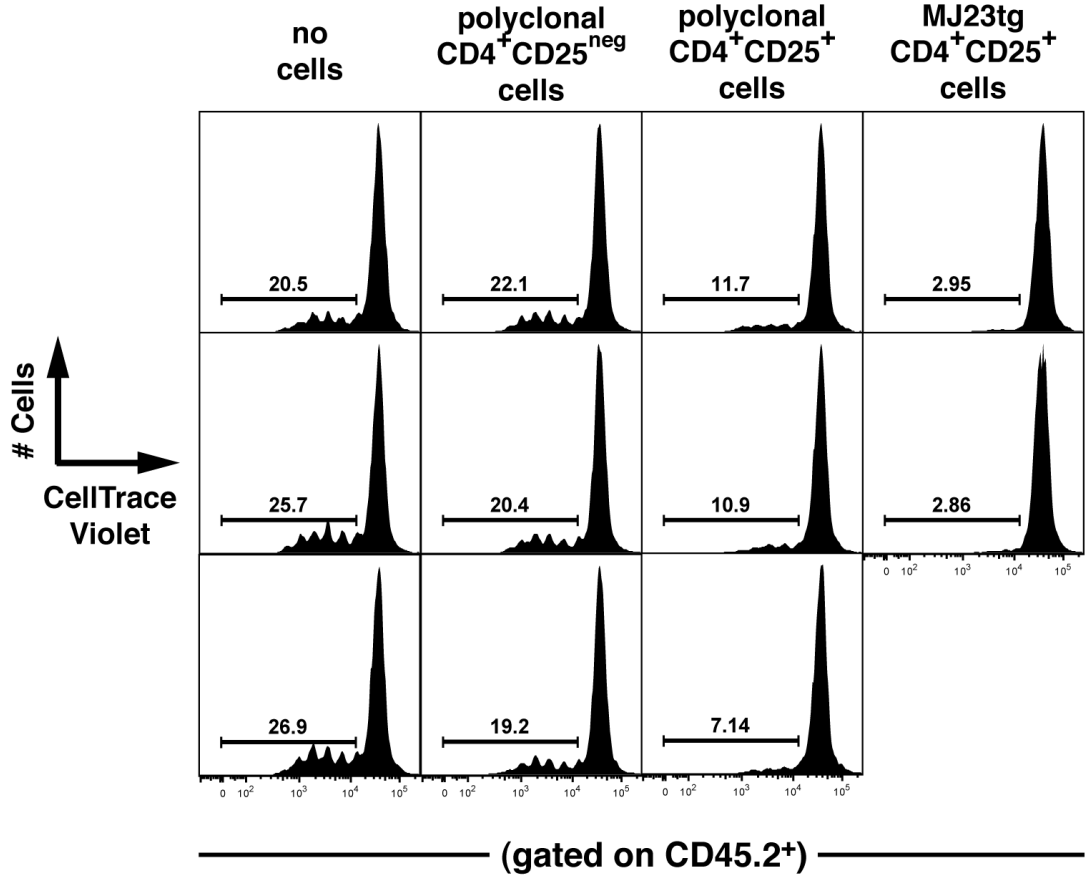

fig. S6. Suppressive function of Tregs from MJ23tg *Rag1*$^{-/-}$ males. Suppressive activity of MJ23tg Tregs *in vitro*. 2.5 x 10^4 polyclonal CD45$^{.2/.2}$CD4$^+$ CD25^{neg} T responder cells labeled with CellTrace-Violet (CTV) were stimulated with 5 x 10^4 irradiated CD45$^{.1/.1}$ splenocytes plus 0.25 μg/mL soluble anti-CD3 antibody. In addition, 2.5 x 10^4 of the indicated FACS-purified CD45$^{.1/.1}$ cells were added to the culture. CD4$^+$CD25$^+$ MJ23tg cells were isolated from the prostates of male MJ23tg *Rag1*$^{-/-}$ mice. CD4$^+$CD25$^+$ polyclonal cells were isolated from the spleen and lymph nodes of B6.SJL mice. Dilution of CTV was assessed by flow cytometry at day 4. The percentage of CD45.2$^+$ T responder cells with diluted CTV is indicated.

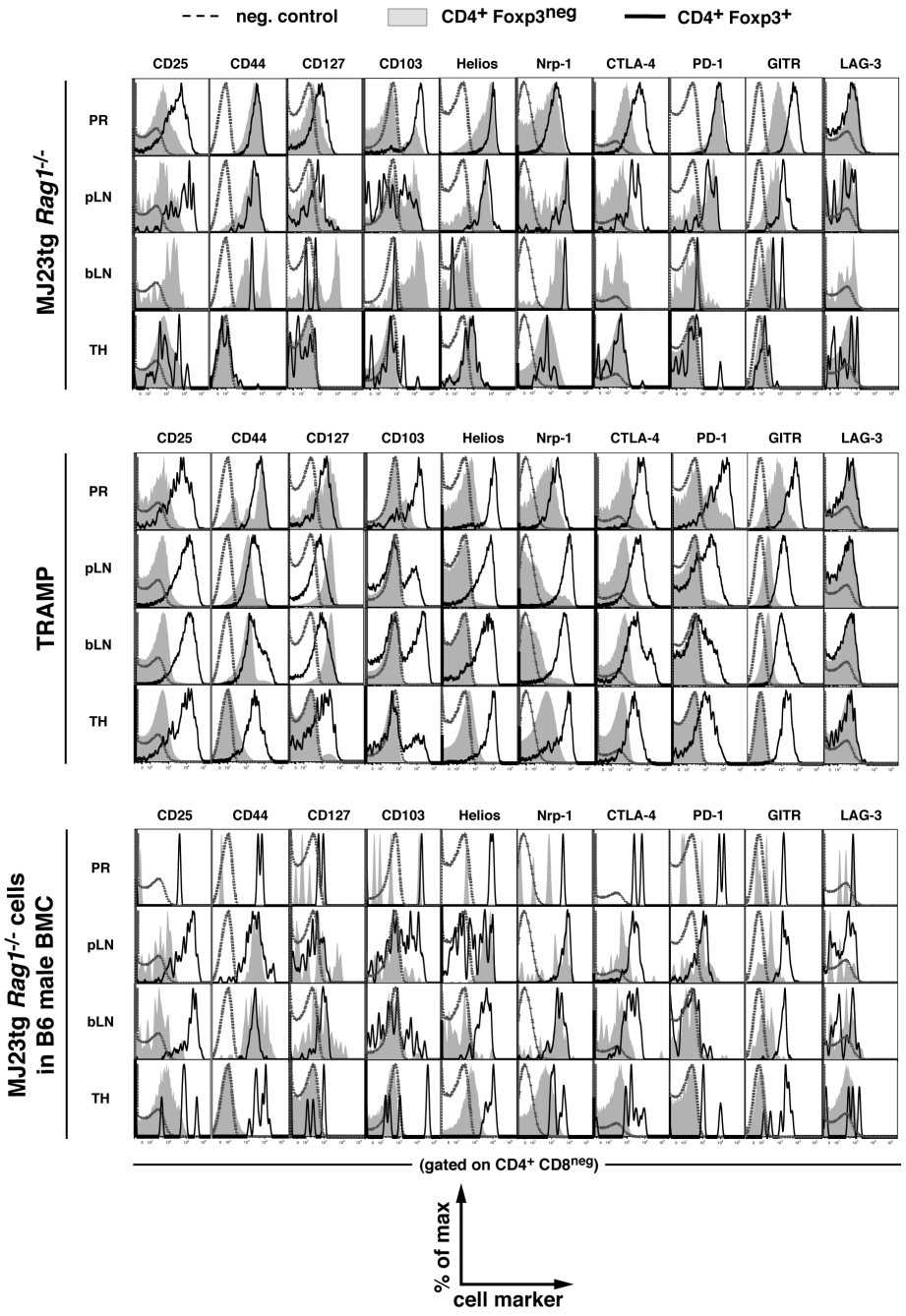

fig. S7. Phenotypic analysis of MJ23tg Tregs. Representative flow cytometric analysis of $CD4^+$ T cells from the prostate (PR), periaortic lymph nodes (pLN), brachial lymph nodes (bLN), and thymus (TH) of the indicated mice. The cells analyzed are as follows: Top, T cells pooled from 12-week-old MJ23tg *Rag1*$^{-/-}$ males; Middle, polyclonal T cells pooled from 27-week-old TRAMP males; Bottom, $CD45.1^+$ MJ23tg donor cells pooled from MJ23tg bone marrow chimeras (BMCs) generated in B6 male hosts. Histogram overlays depict expression of the indicated marker by $CD4^+Foxp3^{neg}$ and $CD4^+Foxp3^+$ T cells.

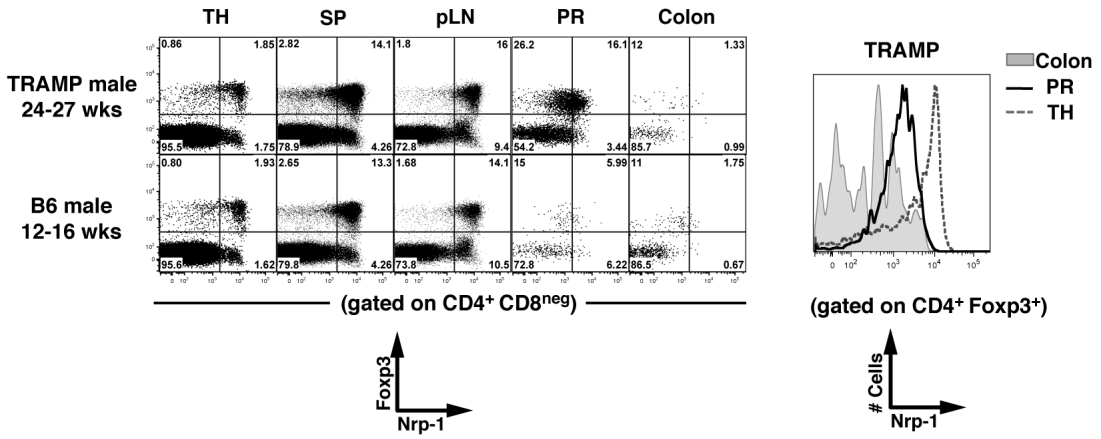

fig. S8. Polyclonal Tregs from TRAMP prostates express intermediate amounts of neuropilin-1. Flow cytometric analysis of $CD4^+$ T cells isolated from different organs of 24-27-week-old TRAMP or B6 males. Left, plots of Foxp3 vs. neuropilin-1 (Nrp-1) expression are shown. The percentage of cells within each quadrant is indicated. Right, histograms of Nrp-1 expression are shown for $Foxp3^+$ cells from the indicated organs of a TRAMP mouse.

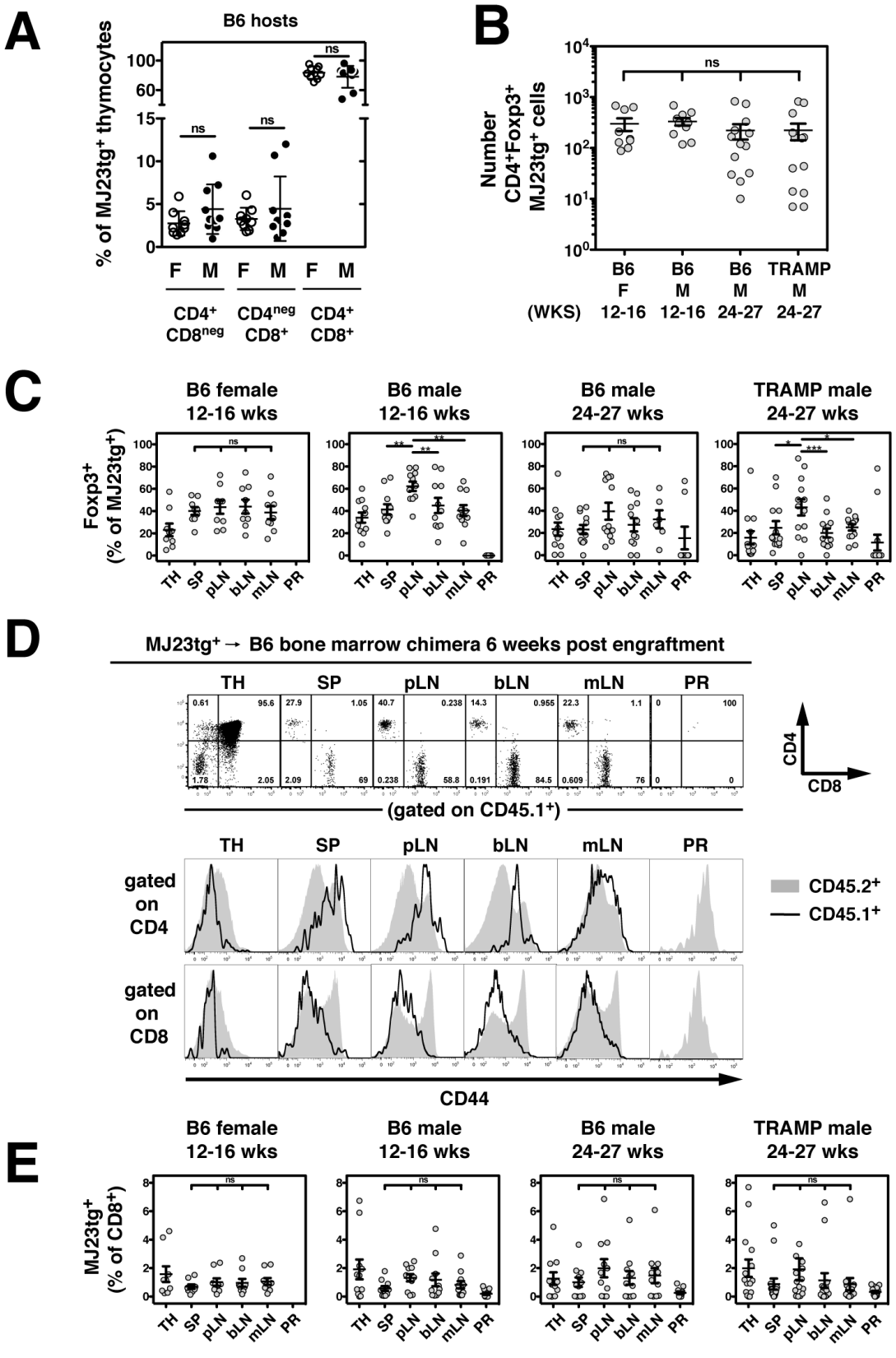
A
B6 hosts
% of MJ23tg+ thymocytes
ns
F M F M F M
CD4+ CD8neg
CD4neg CD8+
CD4+ CD8+
B
Number CD4+Foxp3+ MJ23tg+ cells
B6 F 12-16
B6 M 12-16
B6 M 24-27
TRAMP M 24-27
(WKS)
C
B6 female 12-16 wks
B6 male 12-16 wks
B6 male 24-27 wks
TRAMP male 24-27 wks
Foxp3+ (% of MJ23tg+)
TH SP pLN bLN mLN PR
D
MJ23tg+ → B6 bone marrow chimera 6 weeks post engraftment
TH SP pLN bLN mLN PR
CD4
CD8
(gated on CD45.1+)
gated on CD4
gated on CD8
CD45.2+
CD45.1+
CD44
E
B6 female 12-16 wks
B6 male 12-16 wks
B6 male 24-27 wks
TRAMP male 24-27 wks
MJ23tg+ (% of CD8+)

fig. S9. Additional characterization of MJ23tg bone marrow chimeric mice. Data are from the same mice depicted in Fig. 3. T cell-depleted bone marrow cells from MJ23tg *Rag1*$^{-/-}$ CD45.1^{+} female donor mice were engrafted, along with polyclonal "filler" cells from B6 females (CD45$^{.2/.2}$), into sublethally irradiated CD45$^{.2/.2}$ recipient mice. This approach resulted in seeding of MJ23tg precursors at a low frequency (<1%). 6 weeks post-engraftment, the fate of MJ23tg cells was analyzed. **(A)** Summary plot of the percentage of CD45.1^{+} MJ23tg thymocytes that fall within the CD4^{+}CD8^{neg}, CD4^{neg}CD8^{+}, and CD4^{+}CD8^{+} subsets of 12-16-week-old B6 female (F) or male (M) hosts. **(B)** Summary plot of the absolute number of CD4^{+}CD8^{neg}Foxp3^{+}CD45.1^{+} MJ23tg T cells from the thymus of the indicated hosts. **(C)** Both CD4^{+}Foxp3^{neg} and CD4^{+}Foxp3^{+} MJ23tg cells are present in the periphery of chimeric hosts. Summary plots of the percentage of Foxp3^{+} cells amongst CD45.1^{+}CD4^{+} MJ23tg T cells isolated from various organs of the indicated hosts. **(D)** CD8^{+}CD4^{neg} MJ23tg T cells are present in the periphery of chimeric mice, and exhibit an antigen-inexperienced phenotype. Representative flow cytometric analyses of T cells from different anatomical sites of a male chimeric host. Top, plots of CD4 vs. CD8 expression by CD45.1^{+} MJ23tg T cells. Bottom, histogram overlays of CD44 expression by CD4^{+} and CD8^{+} T cells, both CD45.1^{+} MJ23tg cells and CD45.2^{+} polyclonal cells. **(E)** CD8^{+}CD4^{neg} MJ23tg T cells are widely distributed in the periphery of chimeric hosts, and are not significantly enriched in the periaortic lymph nodes. Summary plots of the percentage of CD45.1^{+} MJ23tg T cells amongst all CD8^{+} cells isolated from various organs of the indicated hosts. The mean ± SEM is indicated. Asterisks indicate $p < 0.05$. For A, a t-test was used to compare male vs. female of the indicated thymic subsets. For B, ANOVA was used to compare the four groups. For C and E, ANOVA was used to compare the secondary lymphoid sites (spleen and lymph nodes) within chimeric hosts of a given type. Abbreviations are the same as in Fig. 2. Data are pooled from at least $N = 3$ independent experiments.

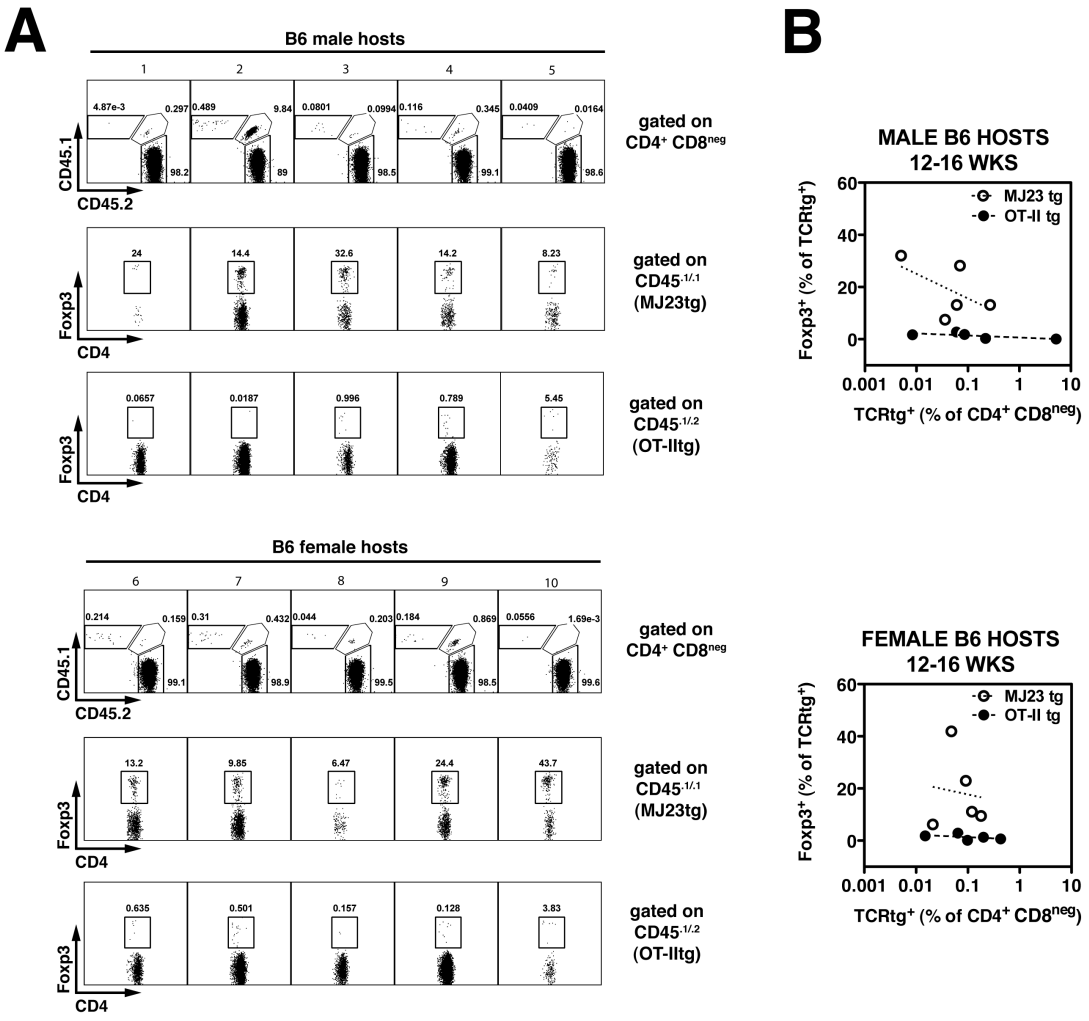

fig. S10. The OT-II TCR does not facilitate Treg development in the thymus of mixed bone marrow chimeric mice. T cell-depleted bone marrow cells from MJ23tg *Rag1*$^{-/-}$ CD45$^{.1/.1}$ female and OT-IItg *Rag1*$^{-/-}$ CD45$^{.1/.2}$ female mice were engrafted, along with polyclonal "filler" cells from B6 females (CD45$^{.2/.2}$), into sublethally irradiated B6 male or female (CD45$^{.2/.2}$) recipient mice. Donor cell proportions were 5% MJ23tg, 5% OT-IItg, and 90% B6 filler. This approach resulted in seeding of MJ23tg and OT-IItg precursors at a low frequency (<1%). 6 weeks post-engraftment, the fate of donor cells was analyzed. **(A)** Representative flow cytometric analyses of CD4^{+}CD8^{neg} thymocytes from the indicated hosts. Plots of CD45.1 vs. CD45.2 depict undepleted thymus samples. Plots of Foxp3 vs. CD4 depict CD8-depleted thymus samples. The percentage of cells within the indicated gates is shown. **(B)** Summary plots of the "efficiency" of Treg development, in which the percentage of CD4^{+}CD8^{neg} TCRtg^{+} (MJ23tg or OT-IItg) cells that express Foxp3 is plotted vs. the frequency of TCRtg^{+} thymocytes (as a percentage of all CD4^{+}CD8^{neg} cells) for cells isolated from the indicated hosts. Dashed lines indicate best-fit semi-log curves.

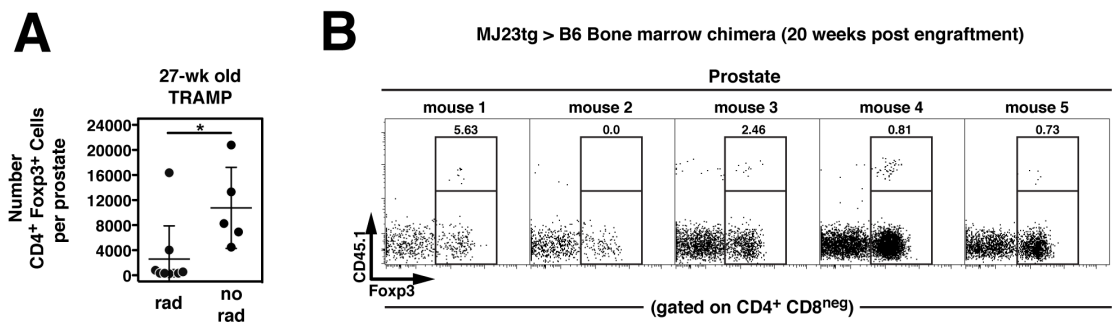

fig. S11. Factors limiting the recovery of donor-derived MJ23tg T cells in chimeric mice. (A) Sublethal radiation substantially reduces the number of Tregs recovered from the prostates of tumor-bearing TRAMP mice. Summary plot of the absolute number of $CD4^+Foxp3^+$ T cells recovered from the prostates of 27-week-old TRAMP mice that had been subjected to 500 rads of radiation (rad) or no radiation (no rad) 6 weeks prior to analysis. **(B)** In MJ23tg bone marrow chimeric mice, donor-derived $CD45.1^+$ MJ23tg T cells are observed in the prostate 20 weeks post-engraftment. MJ23tg chimeras were generated in B6 male hosts as described in Figure 3. Flow cytometric plots of CD45.1 vs. Foxp3 expression are shown for prostatic $CD4^+$ T cells. The percentage of $CD4^+Foxp3^+$ T cells that are $CD45.1^+$ ($MJ23tg^+$) is indicated. The mean ± SEM is indicated. Asterisks indicate $p < 0.05$.

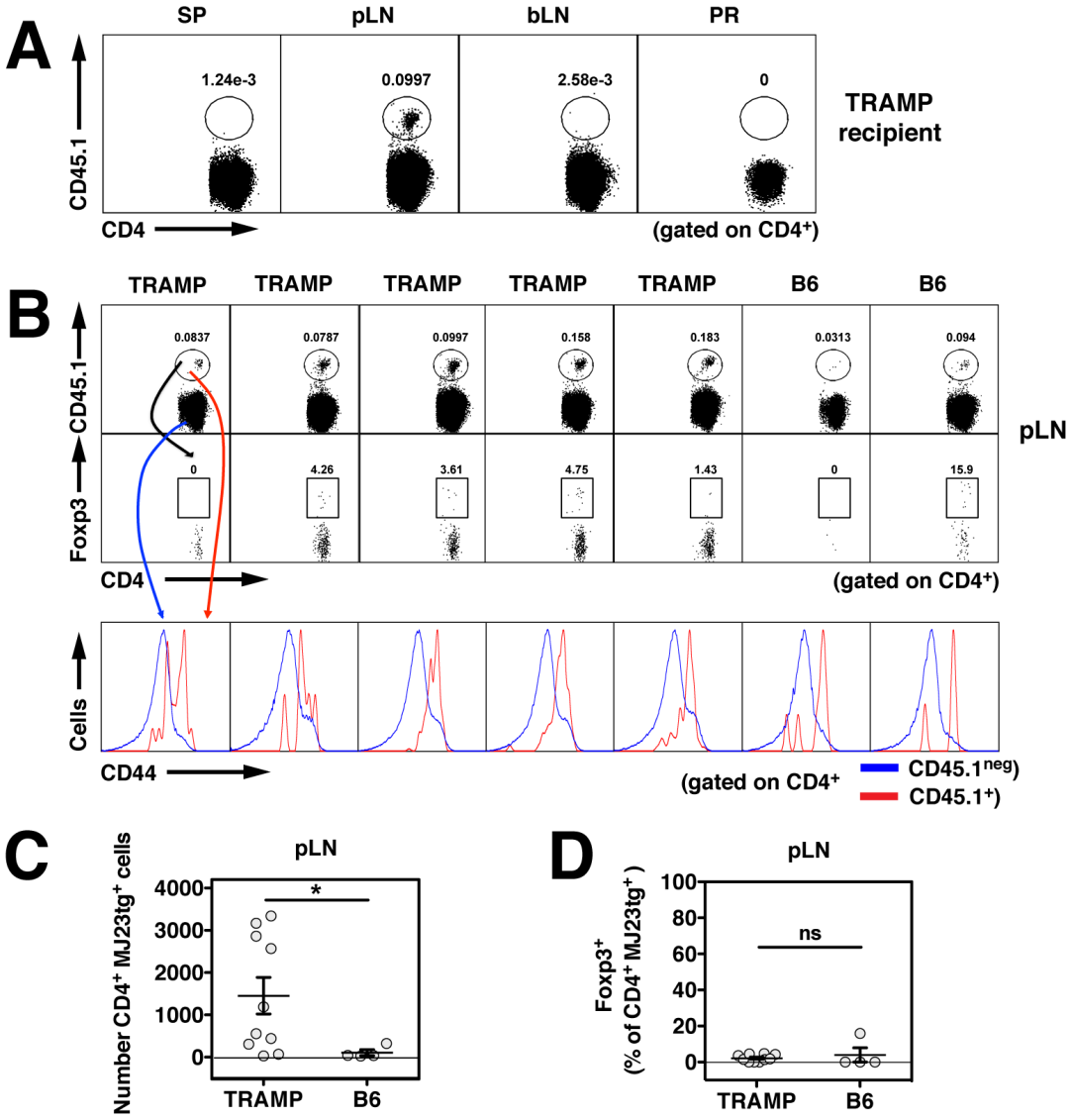

fig. S12. Negligible extrathymic development of MJ23tg Tregs.
1 x 10^5 $CD4^+$ T cells isolated from MJ23tg *Rag1*$^{-/-}$ $CD45.1^+$ female donor mice were transferred intravenously into 5-month-old $TRAMP^{+/+}$ or B6 male recipients. 30 days post-transfer, the fate of donor cells was assessed. **(A)** Representative flow cytometric analysis of the recovery of $CD45.1^+$ MJ23tg donor cells from a TRAMP male recipient, demonstrating that donor cells were exclusively recovered from the periaortic lymph nodes. SP, spleen; pLN, periaortic lymph nodes; bLN, brachial lymph nodes; PR, prostate. **(B)** Representative flow cytometric analysis of $CD45.1^+$ MJ23tg donor T cells in the pLN of the indicated recipient mice. Arrows indicate subgating. **(C)** Summary plot of the absolute number of $CD4^+CD45.1^+$ MJ23tg T cells recovered from the pLN of the indicated recipient mice. **(D)** Summary plot of the percentage of $CD4^+CD45.1^+$ MJ23tg T cells in the pLN that express Foxp3. The mean ± SEM is indicated. Asterisks indicate $p < 0.05$. Data in (C) and (D) are pooled from $N = 2$ experiments.

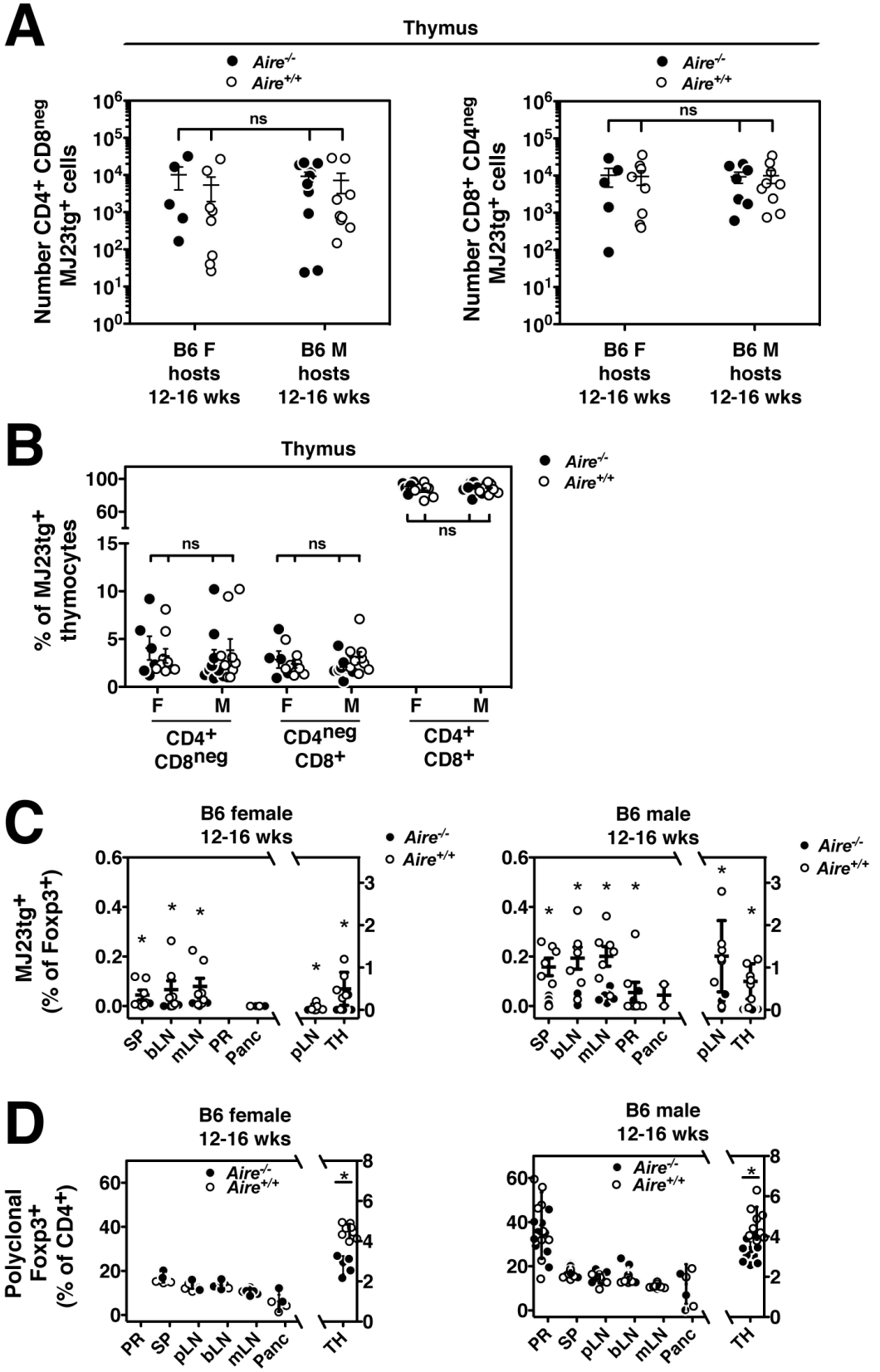
A
Thymus
Aire-/-
Aire+/+
Number CD4+ CD8neg MJ23tg+ cells
Number CD8+ CD4neg MJ23tg+ cells
ns
B6 F hosts 12-16 wks
B6 M hosts 12-16 wks
B
Thymus
% of MJ23tg+ thymocytes
F
M
CD4+ CD8neg
CD4neg CD8+
CD4+ CD8+
C
B6 female 12-16 wks
B6 male 12-16 wks
MJ23tg+ (% of Foxp3+)
SP
bLN
mLN
PR
Panc
pLN
TH
D
B6 female 12-16 wks
B6 male 12-16 wks
Polyclonal Foxp3+ (% of CD4+)

fig. S13. Further characterization of MJ23tg T cells in *Aire*$^{-/-}$ and *Aire*$^{+/+}$ chimeric hosts. Data are from the same mice depicted in Figure 4. T cell-depleted bone marrow cells from MJ23tg *Rag1*$^{-/-}$ CD45.1^{+} female donor mice were engrafted, along with "filler" cells from *Aire*$^{-/-}$ females (CD45$^{.2/.2}$), into sublethally irradiated *Aire*$^{-/-}$ or *Aire*$^{+/+}$ recipient mice (CD45$^{.2/.2}$), both male and female. 6 weeks post-engraftment, the fate of MJ23tg cells was analyzed. **(A)** The absolute number of thymic CD4^{+}CD8^{neg} and CD8^{+}CD4^{neg} MJ23tg cells is not significantly altered in *Aire*$^{-/-}$ hosts. Summary plots of the absolute number of MJ23tg T cells of the indicated phenotypic subset in the thymus of 12-16-week-old female or male hosts of the indicated genotype. **(B)** The distribution of thymic MJ23tg phenotypic subsets is not significantly altered in *Aire*$^{-/-}$ hosts. Summary plot of the percentage of CD45.1^{+} MJ23tg thymocytes that fall within the CD4^{+}CD8^{neg}, CD4^{neg}CD8^{+}, and CD4^{+}CD8^{+} subsets of female (F) or male (M) hosts of the indicated genotype. **(C)** MJ23tg Treg development is Aire-dependent. Summary plots of the percentage of CD45.1^{+} MJ23tg T cells amongst all CD4^{+}Foxp3^{+} cells isolated from various organs of the indicated hosts. **(D)** The frequency of polyclonal Tregs is not altered in the periphery of *Aire*$^{-/-}$ hosts. Summary plots of the percentage of Foxp3^{+} cells amongst all CD45.2^{+} polyclonal CD4^{+} cells isolated from various organs of the indicated hosts. The mean ± SEM is indicated. Asterisks indicate $p < 0.05$, ns = not significant. For (A-B), ANOVA was used to compare the four groups for each phenotypic T cell subset. For (C-D), t-tests were used to compare data from *Aire*$^{-/-}$ vs. *Aire*$^{+/+}$ hosts at the indicated anatomical sites. Data are pooled from $N = 3$ independent experiments.

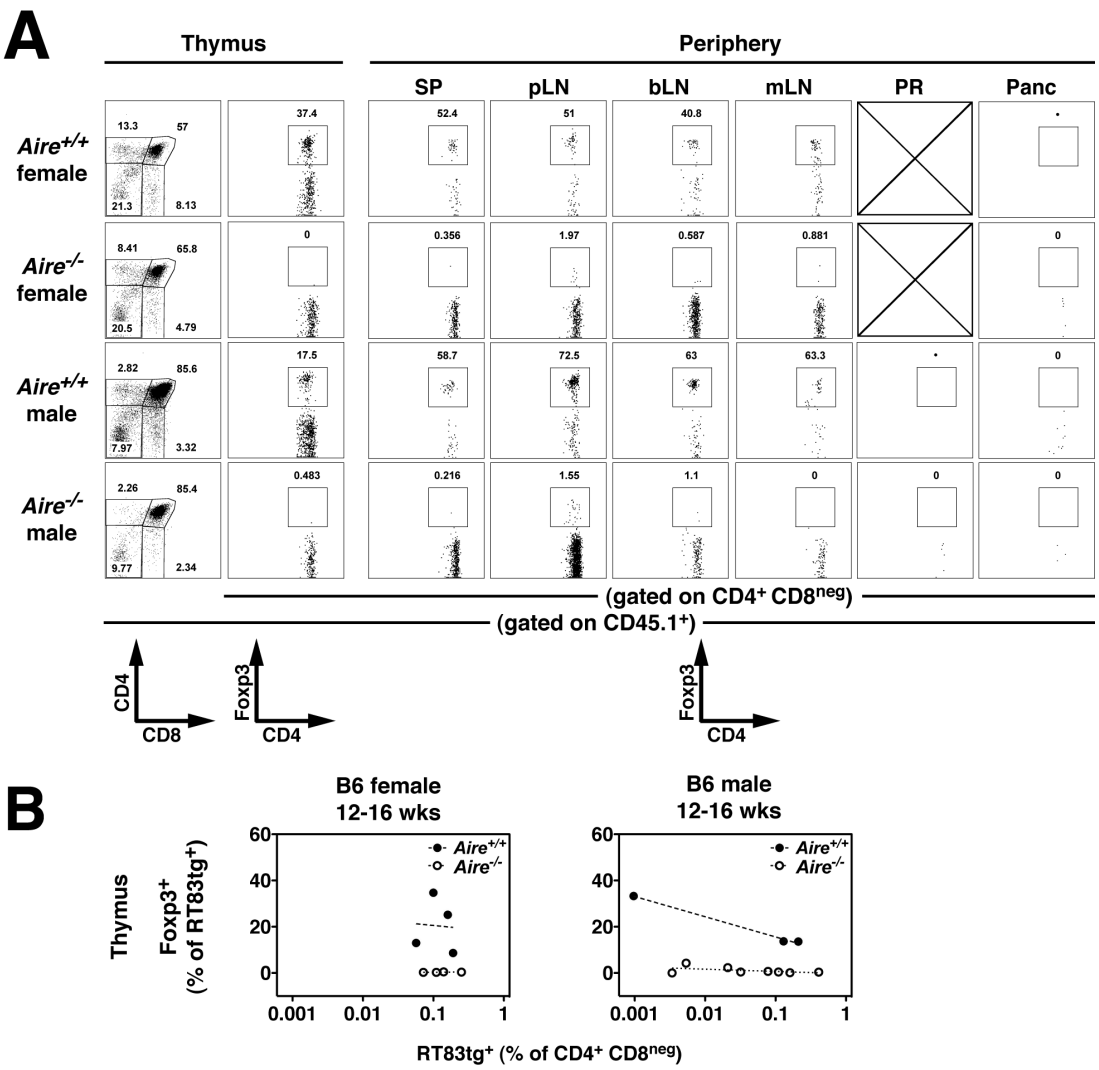
A
Thymus
Periphery
SP
pLN
bLN
mLN
PR
Panc
Aire+/+ female
Aire-/- female
Aire+/+ male
Aire-/- male
13.3
57
21.3
8.13
37.4
52.4
51
40.8
8.41
65.8
20.5
4.79
0
0.356
1.97
0.587
0.881
0
2.82
85.6
7.97
3.32
17.5
58.7
72.5
63
63.3
0
2.26
85.4
9.77
2.34
0.483
0.216
1.55
1.1
0
0
0
(gated on CD4+ CD8neg)
(gated on CD45.1+)
CD4
CD8
Foxp3
CD4
Foxp3
CD4
B
B6 female
12-16 wks
B6 male
12-16 wks
Thymus
Foxp3+
(% of RT83tg+)
Aire+/+
Aire-/-
60
40
20
0
0.001
0.01
0.1
1
RT83tg+ (% of CD4+ CD8neg)

fig. S14. Thymic development of Tregs expressing the "RT83" TCR is Aire-dependent. The RT83 TCRβ chain, Vβ3-ASSLGSSYEQY, was originally identified in polyclonal TRAMP mice based on recurrent expression by prostate tumor-infiltrating Tregs (defined by high-throughput sequencing of $V\beta3^+$ TCRs in fig. S2). The RT83 TCRα chain, Vα8-ALRDSNNRIF, was identified by single cell PCR and sequencing of TCRs expressed by $V\alpha8^+V\beta3^+CD4^+CD25^{high}$ T cells sorted from TRAMP prostate tumors. This analysis identified multiple single cells that co-express the RT83 TCRα and TCRβ chains in polyclonal TRAMP mice (not shown). The RT83 TCRβ chain is the TCR chain expressed by "TCRβtg" mice utilized elsewhere in this study. (A-B) The thymic development of RT83tg Tregs is Aire-dependent. T cell-depleted bone marrow cells from RT83tg *Rag1*$^{-/-}$ $CD45.1^+$ female donor mice were engrafted, along with "filler" cells from *Aire*$^{-/-}$ females ($CD45^{.2/.2}$), into sublethally irradiated *Aire*$^{-/-}$ or *Aire*$^{+/+}$ recipient mice ($CD45^{.2/.2}$), both male and female. 6 weeks post-engraftment, the fate of RT83tg cells was analyzed. **(A)** Representative flow cytometric analyses of $CD45.1^+$ RT83tg T cells from different anatomical sites of 12-16-week-old male or female mice of the indicated *Aire* genotype. Abbreviations are the same as in Fig. 2. The percentage of $CD4^+$ cells that are $Foxp3^+$ is shown. For the thymus, the left column (CD4 vs. CD8) depicts undepleted samples, the right column (Foxp3 vs. CD4) depicts CD8-depleted samples. **(B)** Summary plots of the "efficiency" of RT83tg Treg development, in which the percentage of $CD45.1^+$ RT83tg cells that express Foxp3 is plotted vs. the frequency of $CD45.1^+$ RT83tg thymocytes (as a percentage of all $CD4^+CD8^{neg}$ cells) for cells isolated from host mice of the indicated sex and genotype. Dashed lines indicate best-fit semi-log curves. Data are pooled from $N = 2$ independent experiments.

table S1. Motif table of predicted CDR3 amino acid sequences for $V\alpha2^+$ transcripts expressed by $CD4^+$ T cells from TRAMP prostate tumors. Data are from mice 1-16 depicted in Fig. 1. Analysis of $V\alpha2$ (TRAV14)$^+$ TCRα chains in tumor-bearing $TRAMP^{+/-}$ $Foxp3^{gfp}$ TCRβtg mice. $CD4^+Foxp3^{neg}$ and $CD4^+Foxp3^+$ T cells were FACS-purified from the prostates of ~27-week-old male mice, and cDNA was subjected to deep sequencing. The table lists the number of sequence reads encoding the indicated CDR3 amino acid sequence, for $Foxp3^{neg}$ and $Foxp3^+$ T cells isolated from the indicated mice.

References

1. S. Z. Josefowicz, L. F. Lu, A. Y. Rudensky, Regulatory T cells: mechanisms of differentiation and function. *Annu Rev Immunol* **30**, 531 (2012).
2. M. D. Vesely, M. H. Kershaw, R. D. Schreiber, M. J. Smyth, Natural innate and adaptive immunity to cancer. *Annu Rev Immunol* **29**, 235 (2011).
3. R. J. Deleeuw, S. E. Kost, J. A. Kakal, B. H. Nelson, The Prognostic Value of FoxP3+ Tumor-Infiltrating Lymphocytes in Cancer: A Critical Review of the Literature. *Clin Cancer Res* **18**, 3022 (Jun 1, 2012).
4. N. M. Greenberg *et al.*, Prostate cancer in a transgenic mouse. *Proc Natl Acad Sci U S A* **92**, 3439 (Apr 11, 1995).
5. J. R. Gingrich, R. J. Barrios, B. A. Foster, N. M. Greenberg, Pathologic progression of autochthonous prostate cancer in the TRAMP model. *Prostate Cancer Prostatic Dis* **2**, 70 (Mar, 1999).
6. J. D. Fontenot *et al.*, Regulatory T cell lineage specification by the forkhead transcription factor foxp3. *Immunity* **22**, 329 (Mar, 2005).
7. J. Wong, D. Mathis, C. Benoist, TCR-based lineage tracing: no evidence for conversion of conventional into regulatory T cells in response to a natural self-antigen in pancreatic islets. *J Exp Med* **204**, 2039 (Sep 3, 2007).
8. J. Wong *et al.*, Adaptation of TCR repertoires to self-peptides in regulatory and nonregulatory CD4+ T cells. *J Immunol* **178**, 7032 (Jun 1, 2007).
9. C. S. Hsieh, Y. Zheng, Y. Liang, J. D. Fontenot, A. Y. Rudensky, An intersection between the self-reactive regulatory and nonregulatory T cell receptor repertoires. *Nat Immunol* **7**, 401 (Apr, 2006).
10. S. K. Lathrop, N. A. Santacruz, D. Pham, J. Luo, C. S. Hsieh, Antigen-specific peripheral shaping of the natural regulatory T cell population. *J Exp Med* **205**, 3105 (Dec 22, 2008).
11. Magurran, *Ecological Diversity and Its Measurement*. (Princeton University Press, Princeton, NJ, 1988).
12. M. J. Barnden, J. Allison, W. R. Heath, F. R. Carbone, Defective TCR expression in transgenic mice constructed using cDNA-based alpha- and beta-chain genes under the control of heterologous regulatory elements. *Immunol Cell Biol* **76**, 34 (Feb, 1998).
13. J. L. Bautista *et al.*, Intraclonal competition limits the fate determination of regulatory T cells in the thymus. *Nat Immunol* **10**, 610 (Jun, 2009).
14. M. W. Leung, S. Shen, J. J. Lafaille, TCR-dependent differentiation of thymic Foxp3+ cells is limited to small clonal sizes. *J Exp Med* **206**, 2121 (Sep 28, 2009).
15. M. S. Anderson *et al.*, The cellular mechanism of Aire control of T cell tolerance. *Immunity* **23**, 227 (Aug, 2005).
16. M. S. Anderson *et al.*, Projection of an immunological self shadow within the thymus by the aire protein. *Science* **298**, 1395 (Nov 15, 2002).
17. D. Mathis, C. Benoist, Aire. *Annu Rev Immunol* **27**, 287 (2009).
18. Y. Lei *et al.*, Aire-dependent production of XCL1 mediates medullary accumulation of thymic dendritic cells and contributes to regulatory T cell development. *J Exp Med* **208**, 383 (Feb 14, 2011).
19. K. Aschenbrenner *et al.*, Selection of Foxp3+ regulatory T cells specific for self antigen expressed and presented by Aire+ medullary thymic epithelial cells. *Nat Immunol* **8**, 351 (Apr, 2007).
20. A. Liston, S. Lesage, J. Wilson, L. Peltonen, C. C. Goodnow, Aire regulates negative selection of organ-specific T cells. *Nat Immunol* **4**, 350 (Apr, 2003).

21. R. T. Taniguchi *et al.*, Detection of an autoreactive T-cell population within the polyclonal repertoire that undergoes distinct autoimmune regulator (Aire)-mediated selection. *Proc Natl Acad Sci U S A* **109**, 7847 (May 15, 2012).
22. J. DeVoss *et al.*, Spontaneous autoimmunity prevented by thymic expression of a single self-antigen. *J Exp Med* **203**, 2727 (Nov 27, 2006).
23. V. Kouskoff, K. Signorelli, C. Benoist, D. Mathis, Cassette vectors directing expression of T cell receptor genes in transgenic mice. *J Immunol Methods* **180**, 273 (Mar 27, 1995).
24. Materials and methods are available as supplementary materials in Science Online.
25. V. Kouskoff, K. Signorelli, C. Benoist, D. Mathis, Cassette vectors directing expression of T cell receptor genes in transgenic mice. *J Immunol Methods* **180**, 273 (Mar 27, 1995).
26. M. Yadav *et al.*, Neuropilin-1 distinguishes natural and inducible regulatory T cells among regulatory T cell subsets in vivo. *J Exp Med* **209**, 1713 (Sep 24, 2012).
27. J. M. Weiss *et al.*, Neuropilin 1 is expressed on thymus-derived natural regulatory T cells, but not mucosa-generated induced Foxp3+ T reg cells. *J Exp Med* **209**, 1723 (Sep 24, 2012).
28. A. M. Bilate, J. J. Lafaille, Induced CD4+Foxp3+ regulatory T cells in immune tolerance. *Annu Rev Immunol* **30**, 733 (2012).